Evidence for p-type doping of InN

R.E. Jones,[1,2] , K. M. Yu,[1] S.X. Li,[1,2] W. Walukiewicz,[1] J.W. Ager III,[1] E.E. Haller,[1,2] H. Lu,[3] and W.J. Schaff[3]
1. Materials Sciences Division, Lawrence Berkeley National Laboratory, Berkeley, CA 94720
2. Department of Materials Science and Engineering, University of California, Berkeley, CA 94720
3. Department of Electrical and Computer Engineering, Cornell University, Ithaca, NY 14853

Abstract

The first evidence of successful p-type doping of InN is demonstrated. A range of experimental techniques are used to show that Mg-doped InN films are composed of a p-type bulk region, with a thin n-type inversion layer at the film surface that prevents electrical contact to the bulk material. Capacitance-voltage measurements indicate a net concentration of ionized acceptors below the n-type surface layer. Irradiation with 2 MeV He^+ particles, which has been shown previously to introduce donor defects into InN, is used to convert the bulk of InN:Mg from p- to n-type. The conversion process is well-explained by a model that assumes two parallel conducting layers (the surface and the bulk) in the films. Further evidence for the existence of p-type bulk material is provided by the irradiation-induced recovery of the photoluminescence in InN:Mg. However, the binding energy of the Mg acceptor is still undetermined, and the presence of free holes has not been verified.

Despite more than three decades of research, Indium Nitride (InN) remains the least understood of the group III-nitride compounds. The energy gap of this material was recently discovered to be only 0.7 eV, rather than the previously-accepted 1.9 eV, giving the III-nitride alloy system an exceptionally-wide range of direct band gaps, from InN to AlN (6.2 eV) [1,2]. The narrow bandgap has generated a great interest in InN for applications such as high-efficiency solar cells, light-emitting diodes, laser diodes and high-frequency transistors. The ability to

fabricate both p-type and n-type InN is essential to the realization of these devices; however, only n-type InN has been reported to date.

It is now well understood that the ability to dope a semiconductor material depends on the location of the conduction and the valence band edges relative to the Fermi level stabilization energy (E_{FS}), which is located 4.9 eV below the vacuum level [3]. The well-known difficulties with efficient p-type doping of GaN, AlN and ZnO are the result of the very low positions of the valence band edges with respect to E_{FS} in these materials. For example, the maximum free hole concentration in GaN, which has its valence band edge 2.7 eV below E_{FS}, is about 10^{18} cm^{-3} [4]. Since the valence band edge of InN lies 1.1 eV closer to E_{FS} [5], it might be expected that p-type doping of this material would be easier than p-type doping of GaN. However, p-type conductivity in InN has proven to be difficult to achieve and measure, due to the unusually low position of the conduction band edge (CBE) at 0.9 eV below E_{FS}. The formation energy for a donor species is related to the energy difference between the Fermi level and E_{FS}, and the formation energy is reduced when the Fermi level is below E_{FS} [3]. Thus, native point defects in InN are expected to act as donors, explaining the exceptional propensity for n-type doping. In addition, the surface Fermi energy in InN is found to be pinned at E_{FS} by donor-like surface defects, which creates an n-type accumulation layer at the surface that seems unaffected by chemical or physical treatments [6, 7]. The conductivity of this surface layer has to be considered in any analysis of the electrical properties of InN samples.

In this letter we present a body of data that demonstrates p-type doping of InN with Mg acceptors. The presence of the p-type doping in the bulk of epitaxial films was revealed through a combination of experiments that isolate the effects of the n-type conductivity in the surface accumulation layer. Such techniques provide evidence of a net concentration of acceptors in the

bulk, but are not able to verify the presence of free holes. Thus, the acceptor binding energy of Mg remains unknown, and it is possible that only a small fraction of the acceptors are ionized at room temperature. Still, this first indication of p-type InN to be reported is a significant step toward eventual device applications.

The Mg-doped InN films were grown by molecular-beam epitaxy on c-sapphire substrates with a roughly 200 nm-thick GaN buffer layer [8]. The thickness of the InN layer was nearly 500 nm. Thicknesses were determined from growth parameters and verified by Rutherford backscattering spectrometry. Samples from three different growth runs (denoted GS1547, GS1548 and GS1810) were used, and there was some variation in transport properties among different samples from the same run. The Mg concentration, as measured by secondary ion mass spectroscopy, ranged from $2\text{x}10^{20}$ to $1\text{x}10^{21}$ cm^{-3}. A nominally-undoped InN film was used as a standard for comparison; it was a 2700 nm-thick InN film with a 300 nm-thick GaN buffer layer.

Electrolyte-based capacitance-voltage (CV) measurements were used to evaluate variations of the near-surface charge as a function of depth. The standard CV measurement was not possible, since a reliable Schottky contact to InN has not been demonstrated; all metals investigated to date form ohmic contacts. Instead, as in the similar case of InAs [9], which also has its surface Fermi energy pinned above the conduction band edge, we formed a rectifying contact to InN using an electrolyte (0.2 – 1.0 M NaOH in EDTA). The net charge concentration (N) at the edge of the depletion width was derived from the local slope of the C^{-2} vs. V plot by the standard equation:

$$N = \frac{C^3}{q\varepsilon_{InN} A^2 \, dC/dV}, \qquad (1)$$

where ε_{InN} is the static dielectric constant of InN (a value of $10.5\varepsilon_0$ was assumed [10]), A is the area of the semiconductor-electrolyte interface, and q is the unit charge. The capacitance was measured using a high-frequency AC signal superimposed on the DC voltage (V) applied between the contacts. V was varied between -1.0 V and 0.5 V in order to approximate the change in potential with depth in the near-surface region due to the band bending. We caution that this method gives the free electron distribution rather than the donor distribution close to the surface, unlike the typical CV measurement. The donor atoms are localized on the film surface, but the electron distribution is dictated by the band bending. The voltage was related to the film depth using the standard equation for the depletion width [9]. The maximum probe depth was limited by reverse bias breakdown, and was in the range of 5 to 15 nm.

Free carrier concentration and mobility were measured by a Hall effect system with a 3000 Gauss magnet. Indium contacts were used in van der Pauw configuration. High-energy particle irradiation studies used 2 MeV He^+ particles to produce donor-like point defects; the process has been described elsewhere [7]. Irradiation doses ranged from $1.1x10^{14}$ to $8.9x10^{15}$ He^+ cm^{-2}.

Photoluminescence (PL) signals were generated in the backscattering geometry using the 515 nm line of an argon laser as the excitation source. The signals were dispersed by a one meter double-grating monochromator and detected by a liquid-nitrogen-cooled germanium photodiode.

Figure 1 shows space charge concentration profiles derived from the CV measurements of Mg-doped and undoped InN. In nominally-undoped (n-type) InN, the electron concentration has a maximum near the surface and rapidly decreases deeper into the film, appearing to saturate at a value close to the bulk electron concentration measured by Hall effect. The observed surface

charge accumulation is consistent with Fermi level pinning at E_{FS} [7], as well as the intrinsic surface accumulation revealed by high-resolution electron-energy-loss spectroscopy (HREELS) [6]. Mg-doped InN has an electron accumulation layer similar to undoped films at the surface, but also, uniquely, has a charge depletion layer and then a region of negative space charge (as evidenced by a change in the sign of $\frac{\partial(C^{-2})}{\partial V}$) that is attributed to ionized shallow acceptors. From the net concentration of ionized acceptors, we infer a bulk Mg doping level in the low-10^{19} cm^{-3} range. This suggests that between one and 10 percent of the Mg dopant atoms act as acceptors. The inset of Fig. 1 shows the band diagram of Mg-doped InN that is supported by these measurements. An electron accumulation (inversion) layer may also be formed at the interface with the GaN buffer layer, but this has not been proven. It should be noted that the electrolyte-based CV technique causes the ionization of all uncompensated acceptors in the film, which is not necessarily the concentration that is ionized at room temperature. Thus, the inferred bulk doping level may not indicate the concentration of free holes.

The sheet concentrations of free electrons in the Mg-doped samples, as determined from Hall effect measurements, ranged from $5x10^{13}$ to $7x10^{14}$ cm^{-2}, and electron mobilities from 15 to 90 $cm^2/V{\cdot}s$. If the films were entirely n-type, then the average electron concentrations would range from $1x10^{18}$ to $1x10^{19}$ cm^{-3}. However, the electron mobilities (15 to 90 $cm^2/V{\cdot}s$) are roughly one order of magnitude lower than those of undoped InN at similar electron concentrations. Instead, the mobility values of these Mg-doped samples fall within the range spanned by undoped films with electron concentrations in the mid-10^{20} cm^{-3} [11]. This discrepancy can be explained in terms of the band diagram of Mg-doped InN (Fig. 1 inset). The electron inversion layer that results from the pinning of the surface Fermi energy at 0.9 eV above the conduction band edge is electrically isolated from the p-type bulk material by a depletion

region. Consequently, the inversion layer determines the electrical properties measured by the Hall effect. Assuming a thickness of several nm (as indicated by CV measurements), these inversion layers have electron concentrations on the order of 10^{20} cm^{-3}. Thus, the electron mobility values in these layers are comparable to those in undoped InN films with bulk electron concentrations of this magnitude.

To further investigate the p-type activity of Mg-doped InN, we irradiated the films with 2 MeV He^+ particles. We have shown recently that He^+ irradiation can be used to predictably increase the electron concentration in InN. The irradiation introduces donor defects with energy levels in the conduction band, due to the position of E_{FS} [7]. In undoped InN, the increase in electron concentration is proportional to the irradiation dose, and the electron mobility, which is limited by ionized defect scattering, decreases with dose [11].

The Mg-doped samples show a strikingly different behavior, as depicted in Figs. 2 and 3. At 2 MeV He^+ doses below mid-10^{14} cm^{-2}, the rate of increase in electron concentration is much less than in undoped InN, and electron mobility remains approximately constant. At higher doses, the electron concentration increases continuously, whereas mobility shows a nonmonotonic dependence on the irradiation dose. This behavior is especially evident in sample GS1810, which has the lowest Mg content as determined by SIMS. The He^+ dose of 4.5×10^{14} cm^{-2} generates sufficient donor defects to just overcompensate the electrically-active Mg acceptors and allow n-type transport throughout the film, rather than only in the surface inversion layer. At this point, Hall effect measurements first return electrical properties of the entire film. Upon further irradiation, the properties of the film are controlled by the donor defects and they become comparable to those of the undoped film.

Electron mobility remains low at the p- to n-type conversion threshold because the bulk material is heavily compensated. The mobility in GS1810 shows a distinct maximum near the dose of 1.1×10^{15} He^{+} cm^{-2}, which corresponds to a free electron concentration of 4×10^{19} cm^{-3}. At this point, the electron concentration in the bulk is significantly higher than the concentration of Mg acceptors (i.e. compensation is decreased), while the concentration of ionized defects in the bulk is considerably lower than at the surface. Thus, the measured electron mobility initially increases because of the contribution of the bulk electrons, which see fewer scattering centers than the surface electrons. This maximum less pronounced in GS1547 and GS1548 since the compensation in the bulk is higher due to the larger concentration of ionized acceptors. With additional irradiation, more donor defects are introduced throughout the films and electron mobility decreases correspondingly, as in the undoped sample.

We have modeled the dependence of the electron concentration and mobility (μ) on irradiation dose in sample GS1810 (see insets, Figs. 2 and 3). We considered parallel electron transport in the surface and bulk layers when the bulk was n-type, i.e., after overcompensation of the Mg acceptors by donor defects. We used the standard equations for computing the relative contributions of each layer to the properties determined by the Hall effect [12]:

$$n_{Hall}\mu_{Hall} = n_{surf}\mu_{surf} + n_{bulk}\mu_{bulk} \qquad (2)$$

$$n_{Hall}^{2}\mu_{Hall}^{2} = n_{surf}^{2}\mu_{surf}^{2} + n_{bulk}^{2}\mu_{bulk}^{2}, \qquad (3)$$

where n represents sheet concentration (cm^{-2}). Because of the Fermi level pinning at E_{FS} at the surface, we assumed the contribution from the surface layer to be constant (2×10^{14} electrons cm^{-2} with a mobility of 42 $cm^{2}/V \cdot s$) at the initial experimentally-measured values. It may be noted that these calculations are rather insensitive to the value assumed for the surface concentration. The bulk electron mobility and free carrier concentration depended on the irradiation dose and

were calculated using the data for 2 MeV He^+ irradiation of undoped InN. As seen in the insets of Figs. 2 and 3, the modeling is in a good qualitative agreement with the experimental data.

Finally, we investigated the effect of 2 MeV He^+ irradiation on the photoluminescence (PL) response of undoped and Mg-doped InN. Nearly all undoped InN films deposited using our MBE technique and with electron concentrations less than $2x10^{20}$ cm^{-3} exhibit a PL signal. The PL intensity of these films is very insensitive to the He^+ irradiation and is completely quenched only for 2 MeV He^+ doses of at least $4.5x10^{15}$ cm^{-2}. In contrast, as-grown, Mg-doped films do not exhibit PL. This lack of PL can be attributed in part to a strong electric field caused by the severe band bending in the subsurface region (refer to the Fig.1 inset) that separates photoexcited electrons and holes.

Upon irradiation with a 2 MeV He^+ dose of $1.1x10^{15}$ cm^{-2}, however, a PL signal appeared in the sample with the lowest Mg content, GS1810 (Fig. 4). It is important to note that this is the dose that first produces an n-type bulk layer that is not heavily compensated. The irradiation produces an InN material with PL features analogous to those of undoped n-type InN with a moderate electron concentration. Irradiation with higher doses at first increases the PL signal; however, at the dose $6.7x10^{15}$ cm^{-2} that creates approximately $3x10^{20}$ cm^{-3} electrons, the PL is quenched in a manner similar to that observed in n-type samples. Therefore, the recovery of PL requires that the radiation-induced electron concentration be larger than the acceptor concentration and smaller than roughly $3x10^{20}$ cm^{-3}.

In conclusion, we have shown that the unusual electrical and optical properties of Mg-doped InN can be well-explained assuming a p-type bulk region with a thin, n-type inversion layer at the film surface. A wide range of experimental data, including electrolyte-based CV measurements, transport measurements of as-grown and He^+-irradiated films, and

photoluminescence spectroscopy, are consistent with our model. Theoretical calculations demonstrating satisfactory modeling of these results provide further support. While the quantitative p-type conductivity of the bulk material remains to be evaluated, the achievement of a net concentration of ionized acceptors in InN is a major step toward the fabrication of p-n junctions, and therefore electronic and optoelectronic devices using InN.

This work is supported by the Director, Office of Science, Office of Basic Energy Sciences, Division of Materials Sciences and Engineering, of the U.S. Department of Energy under Contract No. DE-AC02-05CH11231. The work at Cornell University is supported by ONR under contract NO. N000149910936. One of the authors (REJ) thanks the U.S. Department of Defense for current support and the National Science Foundation for previous support through graduate student fellowships.

Figure Captions

Figure 1: Space charge distributions in undoped and Mg-doped InN, as determined from electrolyte-based capacitance-voltage (CV) measurements. The insert is the band diagram of Mg-doped InN, showing the electron inversion layer (shaded). The Fermi energy and the Fermi level stabilization energy (E_{FS}) are included.

Figure 2: Electron concentration, measured by Hall effect, as a function of the 2 MeV He^+ dose in the three Mg-doped films, as well as an undoped InN film. The inset shows the experimental data for one Mg-doped film (GS1810) with calculated values derived from our model.

Figure 3: Electron mobility, measured by Hall effect, as a function of the 2 MeV He^+ dose in the three Mg-doped InN films, as well as an undoped InN film. The inset shows the experimental data for one Mg-doped film (GS1810) with calculated values derived from our model.

Figure 4: Photoluminescence (PL) spectra of one Mg-doped film (GS1810) as a function of the 2 MeV He^+ dose, showing the onset of PL after a dose of 1.1×10^{15} cm^{-2}, followed by its quenching after a dose of 6.7×10^{15} cm^{-2}.

References

[1] V. Yu. Davydov, A. A. Klochikhin, R. P. Seisyan, V. V. Emtsev, S. V. Ivanov, F. Bechstedt, J. Furthmu¨ller, H. Harima, A. V. Mudryi, J. Aderhold, O. Semchinova, and J. Graul, *Phys. Status Solidi B* **229**, R1 (2002).

[2] J. Wu, W. Walukiewicz, K.M. Yu, J.W. Ager III, E.E. Haller, H. Lu, W.J. Schaff, Y. Saito, Y. Nanishi, *Appl. Phys. Lett.* **80**, 3967 (2002).

[3] W. Walukiewicz, Physica B **302** 123 (2001).

[4] H. Obloh, K. H. Bachem, U. Kaufmann, M. Kunzer, M. Maier, A. Ramakrishnan, and P. Schlotter, J. Cryst. Growth **195**, 270 (1998).

[5] J. Wu, W. Walukiewicz, K. M. Yu, W. Shan, J.W. Ager III, E.E. Haller, H. Lu, W. J. Schaff, W. K. Metzger, and Sarah Kurtz, J. Appl. Phys. **94**, 6477 (2003).

[6] I. Mahboob, T. D. Veal, C. F. McConville, Hai Lu, and W. J. Schaff, Phys. Rev. Lett. **92**, 36804 (2004).

[7] S.X. Li, K.M. Yu, J. Wu, R.E. Jones, W. Walukiewicz, J.W. Ager III, W. Shan, E.E. Haller, H. Lu, and W. J. Schaff, Phys. Rev. B **71** (16), 161201 (2005).

[8] H. Lu, W.J. Schaff, J. Hwang, H. Wu, W. Yeo, A. Pharkya, and L.F. Eastman, Appl. Phys. Lett. **77** (2000) 2548.

[9] V. Gopal, E.-H. Chen, E. P. Kvam, and J. M. Woodall, J. Electronic Materials 29, 1333 (2000).

[10] T. Inushima, M. Higashiwaki, T. Matsui, Phys. Rev. B **68**, (2003) 235204.

[11] R.E. Jones, S.X. Li, L. Hsu, K.M. Yu, W. Walukiewicz, Z. Liliental-Weber, J.W. Ager III, E.E. Haller, H. Lu and W.J. Schaff, Physica B (in press).

[12] R.L. Pertritz, Phys. Rev. **110**, 1254 (1958).

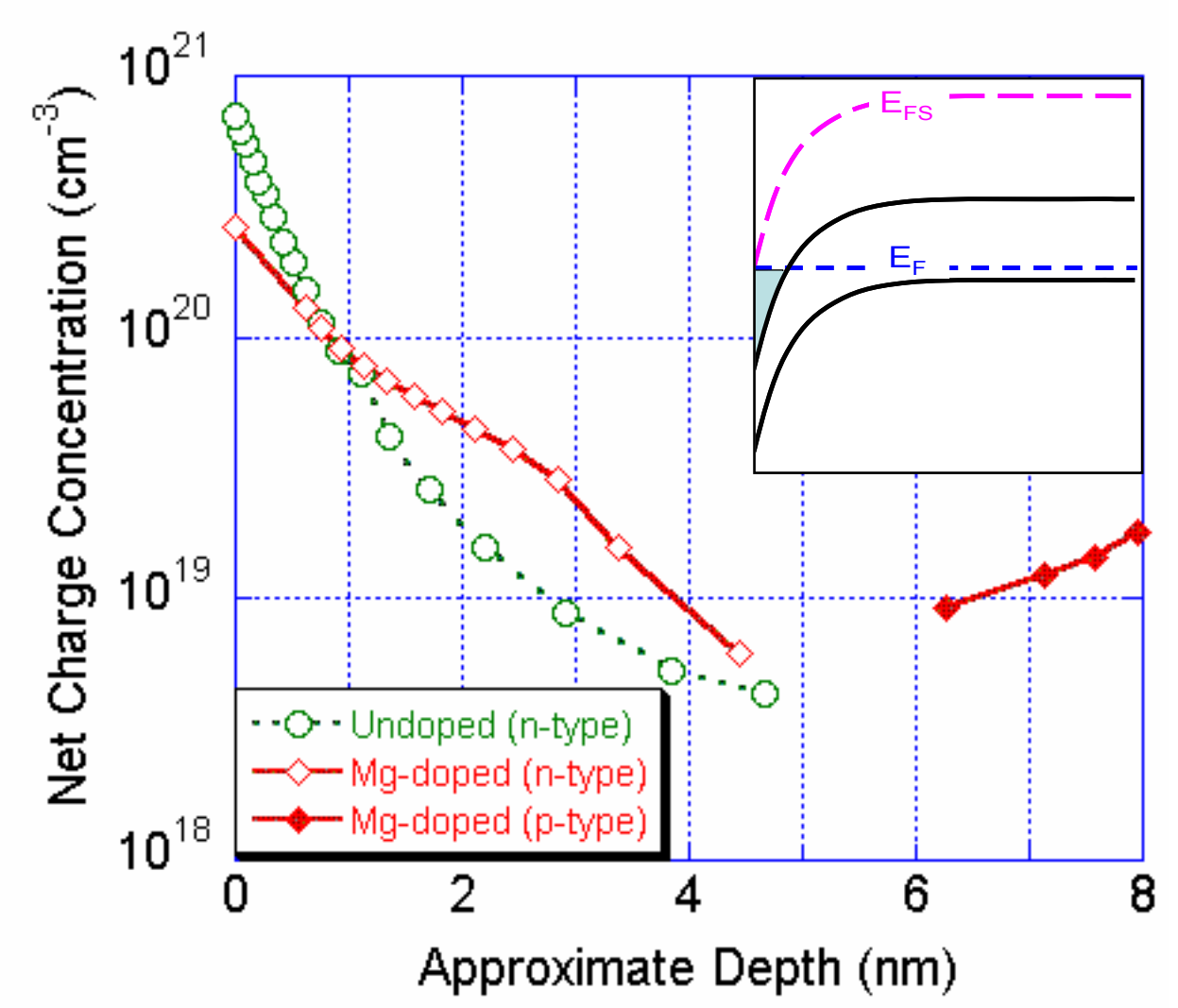
Net Charge Concentration (cm^{-3})
10^{21}
10^{20}
10^{19}
10^{18}
0
2
4
6
8
Approximate Depth (nm)
Undoped (n-type)
Mg-doped (n-type)
Mg-doped (p-type)
E_{FS}
E_F

Figure 1

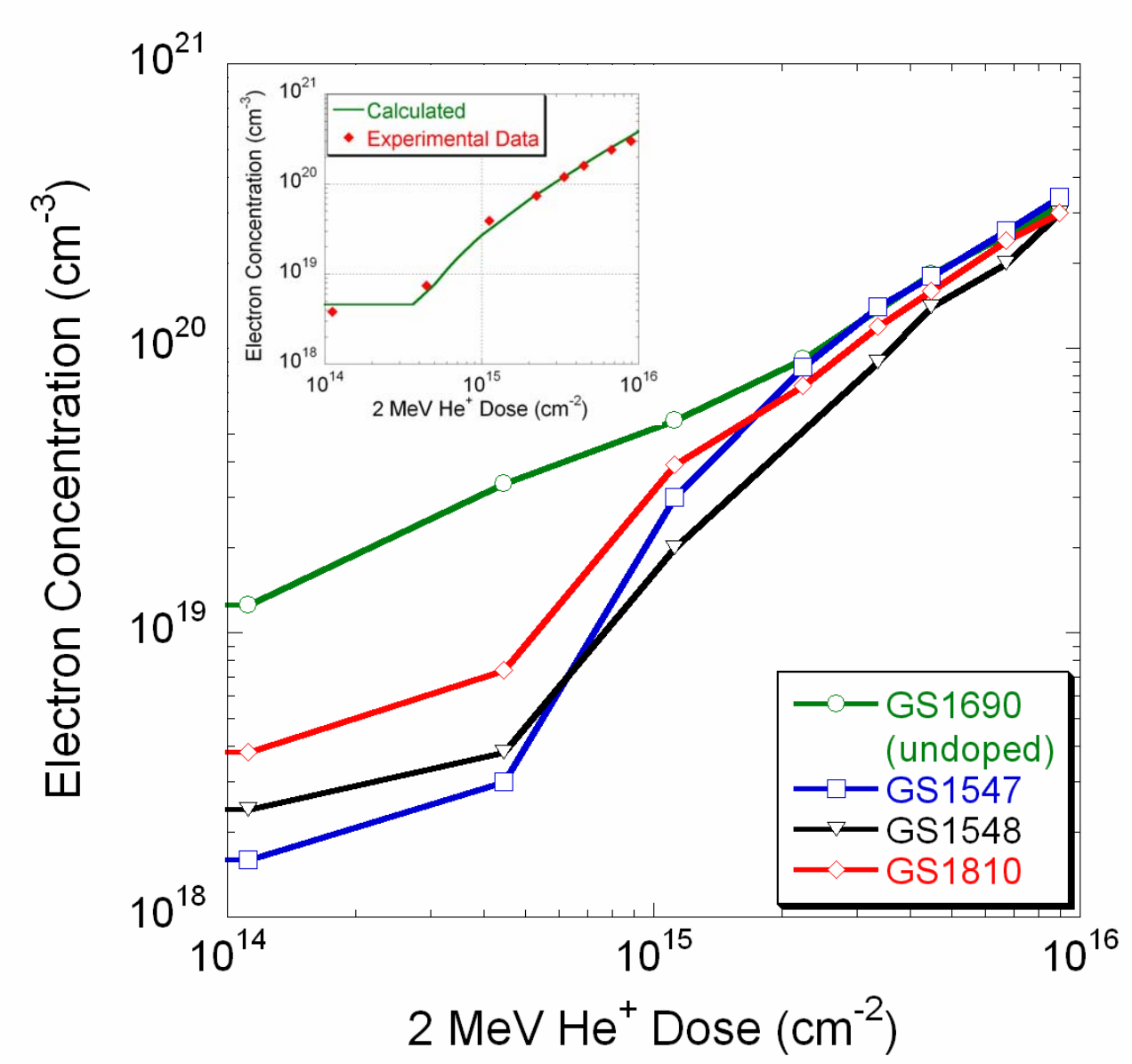
Electron Concentration (cm-3)
2 MeV He+ Dose (cm-2)
GS1690 (undoped)
GS1547
GS1548
GS1810
Calculated
Experimental Data

Figure 2

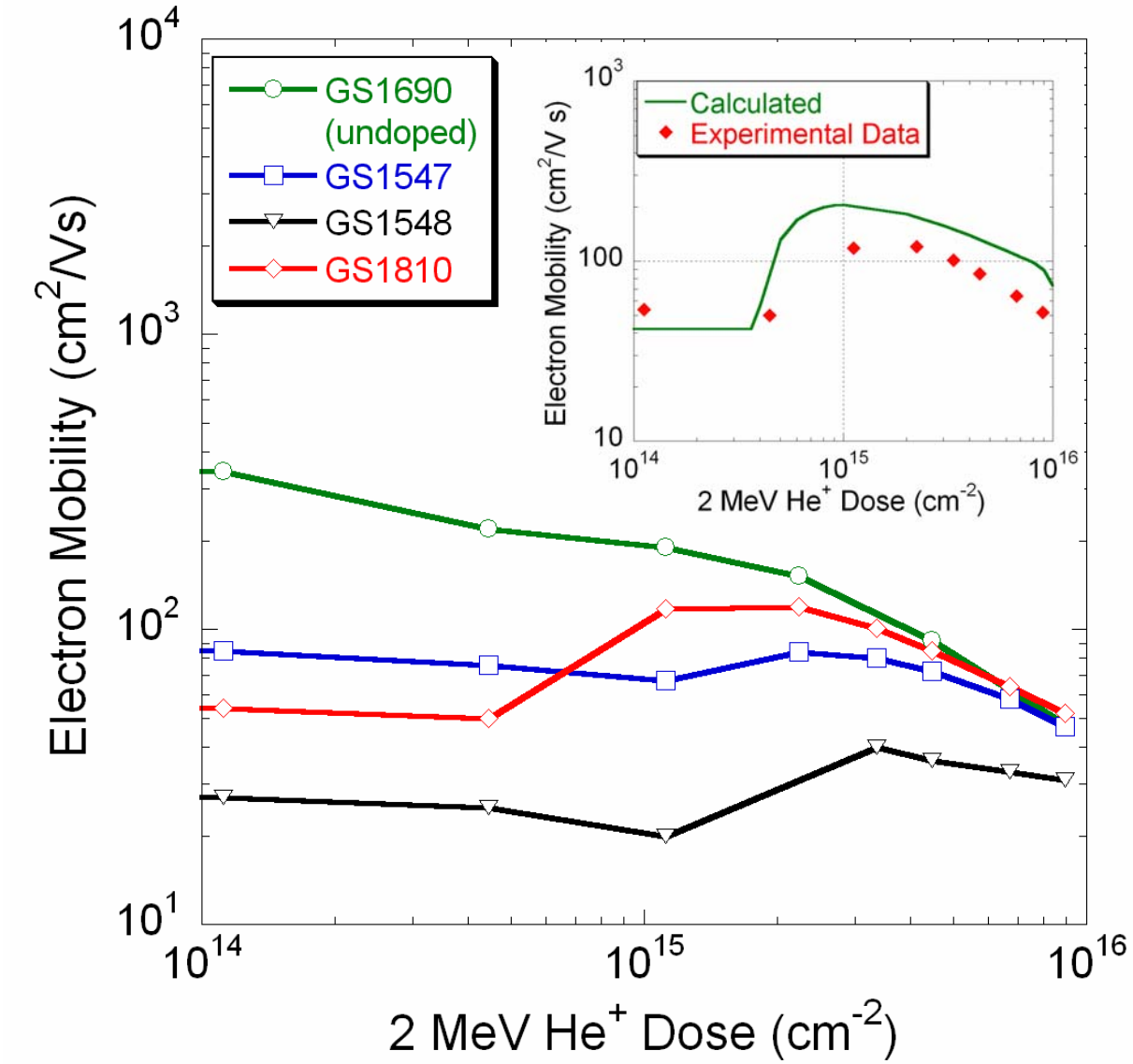
GS1690
(undoped)
GS1547
GS1548
GS1810
Electron Mobility (cm²/Vs)
2 MeV He⁺ Dose (cm⁻²)
Calculated
Experimental Data
Electron Mobility (cm²/V s)
2 MeV He⁺ Dose (cm⁻²)

Figure 3

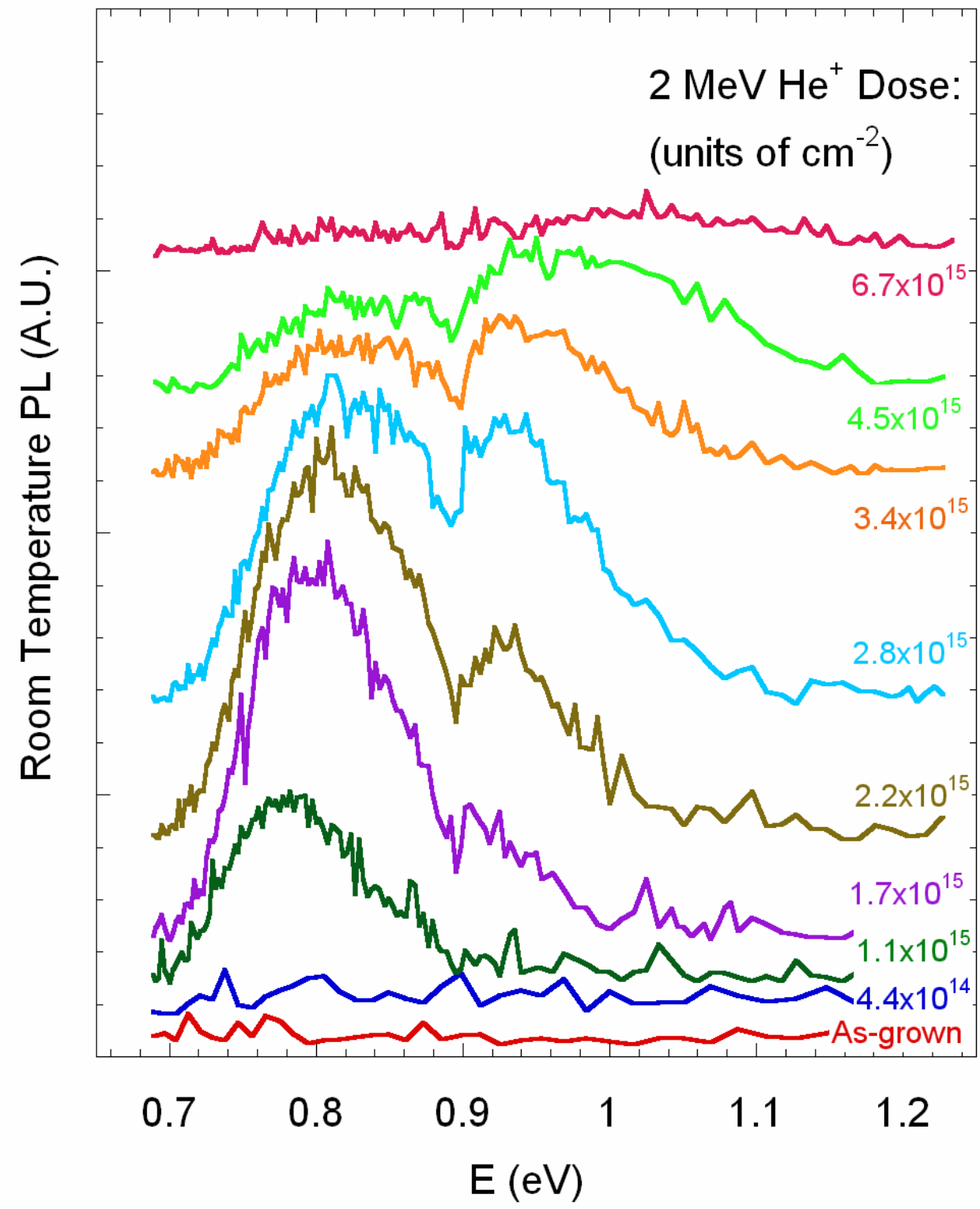
2 MeV He+ Dose:
(units of cm-2)
6.7x10^15
4.5x10^15
3.4x10^15
2.8x10^15
2.2x10^15
1.7x10^15
1.1x10^15
4.4x10^14
As-grown
Room Temperature PL (A.U.)
0.7
0.8
0.9
1
1.1
1.2
E (eV)

Figure 4